NTNU – Trondheim
Norwegian University of
Science and Technology

Calibration of Optical Power with Temperature Sensor

Bastian Fjermeros

June 2014

MASTER THESIS

Department of Electronics and Telecommunications

Norwegian University of Science and Technology

Supervisor 1: Jarle Gran

Supervisor 2: Johannes Skaar

Preface

This assignment was assigned to me by Jarle Gran at the Norwegian Metrology Service (Justervesenet). After doing my project with Justervesenet and Jarle it was an easy choice when I was offered to do my Master with them as well. I started at the Master of Science in electronics programme at NTNU in 2009 and spent my fourth year at the University of Auckland in New Zealand. For the last year I have been situated at Kjeller where I have done my project and now master in cooperation with Justervesenet. The master was carried out during the spring of 2014 and the work was done at the Justervesenet premises in Kjeller and in my office at UNIK.

Kjeller, 2014-06-16

Bastian Fjermeros

Acknowledgement

I want to thank first of all Jarle Gran and Chi Kwong Tang at Justervesenet for their guidance, knowledge and patience. Also a big thanks to Johannes Skaar at UNIK/NTNU. I want to thank NTNU and especially UNIK for giving me an office space at Kjeller for the last year. Countless hours of table tennis in the basement and meaningless conversations with my fellow students at UNIK has been much appreciated.

Trondheim has meant a great deal for me. NTNU and especially Samfundet has played a big part in my years in Trondheim and will forever occupy a special place in my heart. My flatmates in 2C Victoria St. East and all the fantastic experiences I had in New Zealand will be treasured dearly.

My family, mum, dad and my sister, deserves the biggest thanks of all. I am very grateful for your support and encouragement over the years.

B.F.

Abstract

In this report a way of calibrating optical power using an electrical substitution radiometer-based system is presented. Utilizing two thermistors as temperature sensors, a photodiode and a custom made electric circuit voltage difference generated by optical power is measured. By allowing optical power to be incident on the photodiode the thermistor experiences a rise in temperature, hence a change in resistance value, and the electric circuit convert this into a voltage difference. By sending electric current through the photodiode and heating it this way, one can compare electric and optical power. Also considering reflection losses from the surface of the photodiode one can find the optical power incident on the photodiode. An laser beam incident on the system was determined to be of 10.5836 mW. The system can measure optical power down to 10^{-7} W.

Contents

Preface i

Acknowledgement ii

Abstract iii

1 Introduction **2**

1.1 Norwegian Metrology Service and Its Role 2

1.2 Radiometry And Photometry 2

1.3 Light Measurement 3

1.3.1 The Photodiode 3

1.3.2 Light Meter 4

1.3.3 Photometer 4

1.3.4 Optical Power Meter 4

1.3.5 Electrically Calibrated Pyroelectric Radiometer 4

1.4 ESR 5

1.5 Principle Of Idea 5

1.6 Applications 7

2 Theory **8**

2.1 The Electric Setup 9

2.2 Sensors 10

2.3 The Instrumentation Amplifier 11

2.3.1 Common Mode Rejection Ratio 12

2.4 The Wheatstone Bridge 13

2.5 Characterizing the Electric Setup 15

2.6 The Diode And Thermal Design 17
2.7 Reflection 19
2.7.1 Calculation of Reflection Coefficient 20
2.7.2 Minimizing Reflection Loss 22
2.8 Noise Analysis 23
2.8.1 Types of Noise 23
2.8.2 Instrumentation Amplifier Noise 25
2.8.3 Noise Calculations For The Setup 26

3 Characterization of the System **28**
3.1 Expectations 28
3.2 Characterization of the System 28
3.2.1 Electric Power Measurements to Generate Table 29
3.2.2 Calibrating Optical Power 33
3.3 Sources of Error 37

4 Discussion **39**
4.1 Noise Reduction 39
4.2 Calibrating Optical Power 41
4.3 Use 44

5 Conclusion **45**
5.1 Future Work 46

Bibliography **47**

A Fitted Curves **49**

Chapter 1

Introduction

1.1 Norwegian Metrology Service and Its Role

This assignment was created by Jarle Gran at the Norwegian Metrology Service (Justervesenet). Justervesenet is a governmental agency who carries the responsibility of the Norwegian metrology infrastructure and for ensuring its national and international acceptance [20]. Justervesenet performs calibration of technical equipment for the state and commercial actors in Norway. They are also involved in research, e.g. the Newstar project - New primary standards and traceability for radiometry. The main goal of the Newstar project is to develop a new primary standard for radiometry which has approximately the same cost and functionality as existing standards, only with higher quality, simplified techniques and less uncertainty. This can be related to e.g. the medical industry where photo-sensors are becoming incorporated into advanced diagnostic equipment. For optimal utilization of the equipment it is necessary that it is properly calibrated to ensure its quality and competitiveness.

1.2 Radiometry And Photometry

When characterizing a light source two terms often appear; radiometry and photometry. Radiometry applies to the full electromagnetic spectrum while photometry applies to the visible part of the spectrum. These two terms are often interchanged since they are two different points of views of the same matter. While radiant power (radiant flux) is measured in watts [W], lumi-

nous power has the unit lumen [lm], with a conversion ratio of 683 lm /W at $540 \cdot 10^{12}$Hz.

Table 1.1: *The table shows the radiometric and photometric quantities and their units [2].*

Radiometric Quantity	**Symbol**	**Unit**	**Photometric Quantity**	**Symbol**	**Unit**
Radiant Energy	Q	[J]	Luminous Energy	Q_v	$[\mathrm{lm} \cdot \mathrm{s}]$
Radiant Flux (Power)	Φ P	[W]	Luminous Flux	Φ_v	[lm]
Irradiance	E	$\left[\frac{\mathrm{W}}{\mathrm{m}^2}\right]$	Illuminance	E_v	$\left[\frac{\mathrm{lm}}{\mathrm{m}^2}\right]$

Converting from radiant power to luminous power one have to take the human eye sensitivity function into account [7]. This function describes average the spectral sensitivity of the human eye.

1.3 Light Measurement

There exists several ways to measure light. Photodiodes and optical meters exists and is widely used. Firstly it is important to address what you want to measure. Irradiance and radiant flux are some of the quantities one may want more knowledge about. There are many devices that measures radiation, these are called radiometers.

1.3.1 The Photodiode

One way of measuring optical power is by the use of a photodiode. It is used to convert incident absorbed photons to an electric current that is measurable. The photodiode has the property that for every absorbed photon with sufficient energy it generates an electron-hole pair that can contribute to the current flow in the photodiode. It is not enough to create an electron-hole pair, the charge carriers must also be transported in a particular direction where the electron-hole pair can be collected. To help the charge carriers move through the photodiode an electric field is needed. A p-n junction generates an electric field. This is why the photodiode very often has a p-n junction. The electric field forces the positive and negative charges in different directions. Collected at the terminals they can contribute to the current flow. By measuring the current through the photodiode one can calculate the number of photons absorbed. The photodiode is

spectrally dependent and this means that the possibility of absorbing a photon depends on the wavelength of the incident light. Read more about photodiodes here [19] and in section 2.6.

1.3.2 Light Meter

A light meter is a device that measures the amount of light incident on a surface. It is commonly used in photography when determining the correct exposure when taking a picture. It comes with a small computer where the user can determine the shutter speed and aperture himself.

1.3.3 Photometer

A photometer measures light intensity (illuminance) and optical properties of solutions and surfaces. It consists of photosensitive elements like photoresistors and photodiodes. Some photometers can also count the number of photons incident rather than measuring incoming flux. This photon counting only works where the illuminance is low.

1.3.4 Optical Power Meter

Optical power meters are most used when investigating fiber optic systems. A typical optical power meter is made up by a calibrated sensor, an amplifier and a display. The sensor consist of a photodiode selected to fit certain wavelengths and input powers. The range of a typical optical power meter is from nW to mW.

1.3.5 Electrically Calibrated Pyroelectric Radiometer

ECPR is an absolute accuracy radiometer transfer standard that supports wavelengths from the visible to mid-IR. It measures optical power and irradiance of free-space sources. Standard preferences on the ECPR can measure power of cw sources from 5 μW to 100 mW with $\pm 1\%$ absolute accuracy. Other options can extend the spectral range up to 20 μm [18].

1.4 ESR

Electrical substitute radiometers are devices that measures optical radiation and compare it to an equal amount of electric power. It works in that way that incident optical power heats up an element. On that element a temperature sensor is present to monitor the temperature rise generated by the absorbed optical power. The element is also connected to a heat sink that has a stable temperature. A separate circuit connected to the elements is turned on when the optical radiation stops. This circuits task is to maintain the same temperature of the element as the optical power did. To do that a current flows through the element and heats it up to the thermal equilibrium generated by the optical radiation. It is common to ignore radiative losses from the element. The main challenge with ESR is to characterize the different loss mechanisms in order to apply the correct amount of electric power to the system that coincide with the power equivalence between optical and electric power. It is desirable that

$$P_o = P_e \tag{1.1}$$

where P_o is optical power and P_e is electric power.

Most versions of ESR has a cryogenic chamber for which the optical radiation enters [5] [16]. Since the temperature is low, less optical energy is needed to generate a temperature rise in the illuminated element.

1.5 Principle Of Idea

The idea is to design a temperature sensor circuit that detects the temperature difference between two sensors (see figure 2.1). The temperature sensors are attached to a photodiode and a reference material respectively. The thought is that an illuminated photodiode will have an increase in temperature and that the sensor will detect this. Using a differential amplifier to amplify difference between the two sensors one can detect the change in temperature. To determine the power of the incident light one can use electric heating of the photodiode as a basis of comparison. Applying an electric current through the photodiode will heat it and one can

easily find the power generated heat via

$$P = I \cdot V \qquad [W] \tag{1.2}$$

From the equation above it is obvious that the power is proportional with the current flow and applied voltage. Heating the photodiode with electric power should be a lossless process, in such a way that all the power consumed is converted to heat up the photodiode with no radiative losses. However, using a laser to heat the photodiode is not a lossless process. The laser beam power may not be very stable and there are reflective losses at the photodiode surface. The power used to heat the photodiode is only the absorbed parts of the laser beam so reflection from the surface must also be considered. Reflection losses are calculable using the Fresnel equations and this is done in section 2.7.1.

The electric circuit design that detects the temperature difference should be as simple as possible. The design and all of the modifications done will be presented at a latter stage in this report.

Another integral part of the total setup is the thermal design. This describes the thermo-mechanical design and how the two sensors are connected through heat transfer. It is important with a good thermal design to avoid temperature fluctuations in the sensors that could cause inaccuracy in the measurements.

The material chosen to act as a reference material is copper. Copper has good thermal conductivity and is easy accessible. To ensure that the sensor experiences the same temperature rise as the photodiode the sensor has been glued on the backside using thermal adhesive. Thermal adhesive has the property that it transfers heat very good and it is widely used in integrated circuits when installing heat sinks.

Instead of a photodiode one can use a black resistor, or just the sensor itself, if the only purpose is to measure thermal changes in the material caused by optical radiation. The advantage with using a photodiode is that one can use it as an actual photodiode to measure lower optical powers. Reflection from the surface is also much more convenient to calculate using a silicon photodiode since the spectral refractive index dependency of silicon is well documented [9].

1.6 Applications

Applications for this system could be calibrating optical power in room temperature with higher powers than one usually can do with photodiodes. For low power regular silicon photodiodes are suitable, but with higher powers over about 1 mW the photodiodes are not linear and not very predictable. They tend to saturate at low powers and are most efficient at certain wavelength bands. This report presents a setup that is applicable at a broad range of wavelengths as it converts all the absorbed energy generated by the light to heat energy. No optical radiation will generate current in the photodiode as the terminals are open during optical measurements. This setup can also be adapted to a certain sensitivity using custom thermal design, using only a low mass piece of silicon as a photodiode making it more susceptible to lower powers.

Chapter 2

Theory

As presented in the introduction the idea is to design a system consisting of an electric circuit and a thermomechanical part that include the sensors, photodiode and reference material.

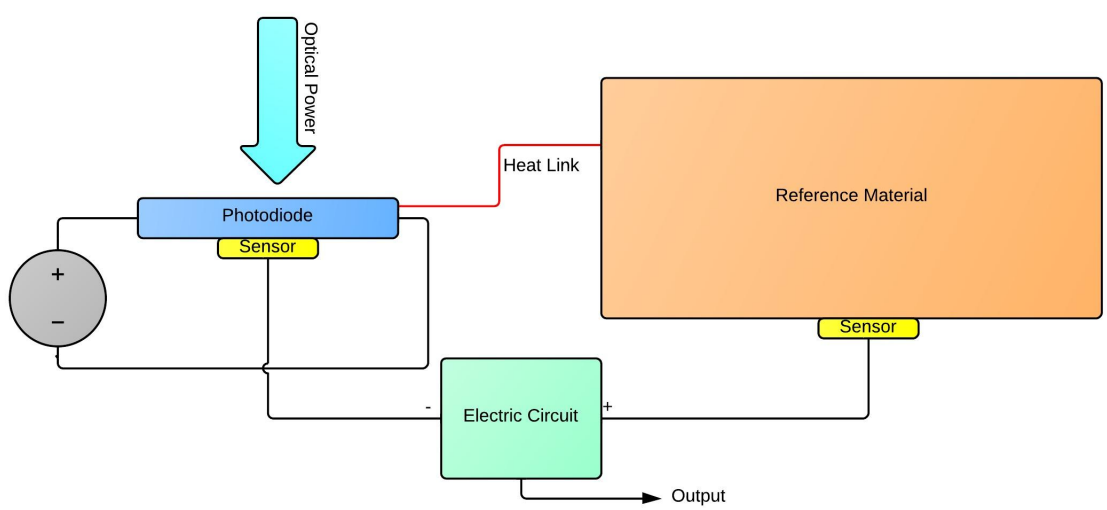

Figure 2.1: *When optical power is incident on the photodiode the power supply is not connected. It is connected when calibrating electrically. The electric circuit contains the instrumentation amplifier and the sensor bridge. The heat link is simply the wiring form the photodiode squeezed between the reference material and a washer.*

As the laser shutter is open the energy from the laser beam will heat the photodiode. After

a while, as the time constants are currently unknown, the temperature will stabilize at a certain level. The temperature difference between the sensors will be represented as a voltage difference between the two sensors. This temperature is determined by the optical power of the laser. After measuring the voltage difference generated by the optical power source one can determine the optical power by applying a voltage that generates the same voltage difference as the optical power. If the power generated electrically generates the same response in the system as the optical power, the optical power is equal to the electric power. But one must remember to consider reflective losses from the surface. The power generated by the voltage source can be found through $P = IV$. To approximate how much electric power is needed to match the optical power one can perform several electrical measurements and create a table before making the optical measurement. The table would be voltage difference on the y-axis and applied power on the x-axis such that each voltage value gives one power value. The table will act only as a tool to find the electric power to apply on the photodiode that will generate a voltage difference above and below the voltage difference generated by the optical power.

2.1 The Electric Setup

To detect the voltage difference generated by optical and electric power an electric circuit is needed. The circuit consists first and foremost of an instrumentation amplifier [3], a sensor bridge and noise reducing capacitors.

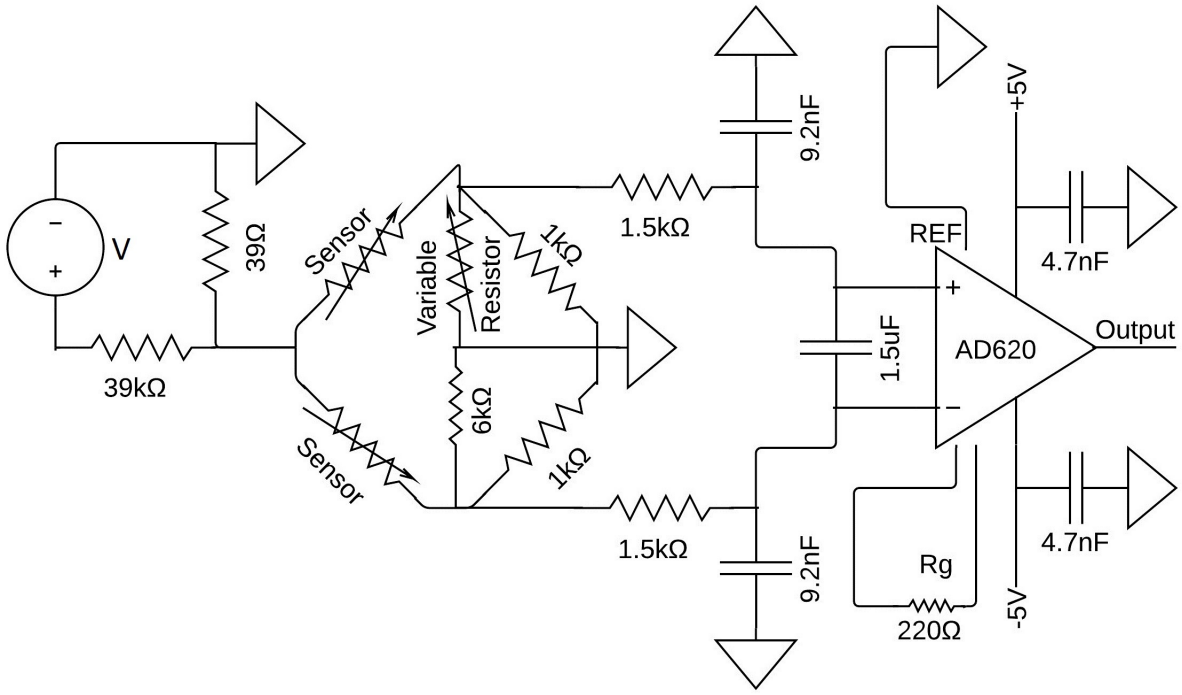

Figure 2.2: *The circuit used in the system. When voltage V is applied current will flow through the bridge making the circuit ready to detect temperature changes in the sensor. As the temperature of the photodiode changes the sensor associated with the photodiode will experience a change in resistance, hence unbalancing the bridge. The temperature change will be represented as a voltage difference between the two sensors. This will be amplified by the instrumentation amplifier AD620. The capacitors are present to reduce noise. For the bridge to be in perfect balance the variable resistor needs to* $6k\Omega$.

The two sensors are thermistors which will be presented in the next section. But they may exhibit different resistance values due to the fact that they are in contact with two different materials. To compensate for that one can simply adjust the variable resistor to reinstall balance in the circuit.

2.2 Sensors

To measure temperature difference two thermistors are used. A thermistor is a temperature sensitive resistor that changes resistance value with temperature. Regular resistor also change

its resistance with temperature but a thermistor is significantly more sensitive. They are widely used as temperature sensors. There are two types of thermistors; resistor value decrease or increase with temperature, called NTC (negative temperature coefficient) and PTC (positive temperature coefficient) respectively. The relationship between temperature and resistance can be expressed as follows:

$$\Delta R = k\Delta T \tag{2.1}$$

where ΔR is the change in resistance, k is the temperature coefficient that determines is the thermistor is NTC-type or PTC-type and ΔT is the temperature change. A usual resistor has a temperature coefficient close to zero.

In this experiment two CX-1070 thermistors from Lakeshore Cryptonics are used [15]. They have a typical resistance of about 66Ω in room temperature (300 K) and has a negative temperature coefficient. The sensitivity is $S = dR/dT = -0.201\Omega/\mathrm{K}$. But the resistance can vary quite widely so separate resistance measurements are recommended [1].

2.3 The Instrumentation Amplifier

The instrumentation amplifier consists of two buffers, one differential amplifier and resistors as shown in figure 2.3. The advantage with this circuit is that one can adjust its amplification by adjusting only one resistor. All the resistor labelled R are equal and R_{gain} is the variable resistor that controls the amplification. The amplification is given by

$$A_v = (1 + \frac{2R}{R_{\text{gain}}}) \tag{2.2}$$

By carefully choosing values for R_{gain} it is easy to control the amplification.

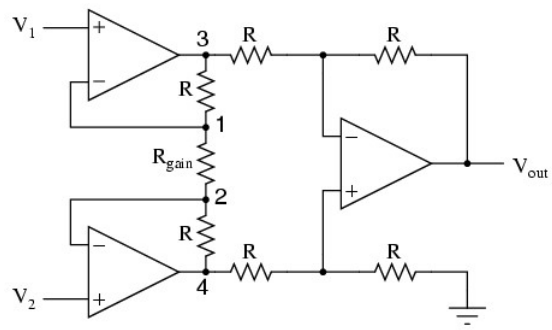

Figure 2.3: *The schematic setup of the instrumentation amplifier.*

A closer look at figure 2.3 will yield a more detailed understanding of its function. The negative feedback of the top left op-amp has no current flow and therefore causes the voltage at point 1 to be equal to V1. Equally, the bottom left op-amp has no current flow, so the voltage at point 2 must be V2. This establishes a voltage drop across R_{gain} equal to $V_2 - V_1$. The current going through R_{gain} must be the same current running through the two resistors above and below R_{gain}. A voltage drop between point 3 and point 4 is created and is equal to:

$$V_{3-4} = (V_2 - V_1)(1 + \frac{2R}{R_{\text{gain}}}) = V_{\text{out}} \tag{2.3}$$

The inputs V1 and V2 have very high impedances and the buffer amplifiers eliminates the need for impedance matching making the instrumentation amplifier a very good tool when used for measurement purposes. In this project the instrumentation amplifier AD620 from Analog Devices is chosen [3].

2.3.1 Common Mode Rejection Ratio

An important feature about the instrumentation amplifier is that it has high common mode rejection ratio. Common mode rejection ratio (CMRR) describes how good the amplifier is to reject unwanted signals that are common to both inputs. Ideally, the CMRR should be infinite such that only the difference between the inputs will be amplified.

$$V_{\text{out}} = G_d(V_+ - V_-) \tag{2.4}$$

where G_d is the differential gain and V_+ and V_- are the input signals. But due to transistor non-idealities some common signal will also be amplified.

$$V_{\text{out}} = G_d(V_+ - V_-) + \frac{1}{2}G_{\text{cm}}(V_+ + V_-) \tag{2.5}$$

Here G_{cm} is the common mode gain which is usually much smaller than the differential gain. CMRR is defined as the ratio of the powers of the differential gain and the common mode gain measured in dB.

$$\text{CMRR} = 20\log\left(\frac{G_d}{|G_{\text{cm}}|}\right) \tag{2.6}$$

2.4 The Wheatstone Bridge

The sensor circuit can be simplified to the Wheatstone bridge as shown in the figure below.

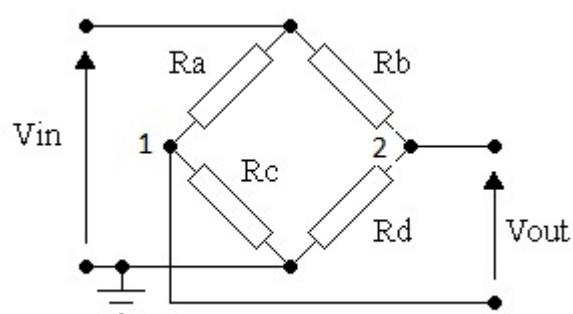

Figure 2.4: *The wheatstone bridge.*

The resistors R_c and R_d could be the combination of a potentiometer and the resistors that make up the circuit. To examine what happens if one of the resistors change value it is necessary to determine when the circuit is balanced, i.e. when the output is zero. It is assumed that the potentiometer of 25 kΩ is perfectly balanced, e.g. with $12.5k\Omega$ on each side of the common ground.

$$V_{\text{out}} = V_1 - V_2 = 0 \tag{2.7a}$$

$$V_1 - V_2 = \frac{V_{in}}{R_a + R_c}R_c - \frac{V_{in}}{R_b + R_d}R_d \tag{2.7b}$$

$$= \frac{R_c}{R_a + R_c} - \frac{R_d}{R_b + R_d} \tag{2.7c}$$

$$= \frac{R_c(\cancel{R_d} + R_b) - R_d(\cancel{R_c} + R_a)}{(R_a + R_c)(R_b + R_d)} \tag{2.7d}$$

$$= \frac{R_c R_b - R_d R_a}{(R_a + R_c)(R_b + R_d)} \tag{2.7e}$$

$$= \frac{\frac{R_b}{R_d} - \frac{R_a}{R_c}}{(\frac{R_a}{R_c} + 1)(\frac{R_b}{R_d} + 1)} \tag{2.7f}$$

The bridge is balanced whenever $\frac{R_a}{R_c} = \frac{R_b}{R_d}$. It is easy to unbalance the circuit by adjusting the potentiometer that determines R_c and R_d. A change in temperature in on of the thermistors R_a or R_b will also unbalance the circuit. In this case the temperature change in one of the thermistors is what is desirable. An early test of the thermistors shows that they have resistance of approximately 90Ω in room temperature. This deviation from the theoretical value presented in section 2.2 is caused by the fact that the resistance values can vary widely as stated here [1]. The thermistors have a typical sensitivity coefficient of $S = dR/dT = -0.201\Omega/\mathrm{K}$ at 300 K. By touching them with the hand for two seconds changes their value by approximately $\Delta\Omega = 1.8\Omega$. The value of R_c and R_d is $1\mathrm{k}\Omega || 12.5\mathrm{k}\Omega = 0.926\mathrm{k}\Omega$. Assuming only R_a changes value we get from the equations above:

$$\frac{\frac{R_b}{R_d} - \frac{R_a - \Delta\Omega}{R_c}}{(\frac{R_b}{R_d} + 1)(\frac{R_a - \Delta\Omega}{R_c} + 1)} = 1.62 \cdot 10^{-3} \tag{2.8}$$

This change gives an indication of how big an impact a temperature change in a balanced circuit would be. A certain ΔΩ will change the voltage output. Using the sensitivity coefficient of the thermistor one can find the voltage sensitivity coefficient for the system:

$$\frac{\Delta \mathrm{V}}{\Delta \mathrm{T}} = 4.4776 \cdot 10^{-3} \qquad \left[\frac{\mathrm{V}}{\mathrm{K}}\right] \tag{2.9}$$

This can be interpreted as the sensitivity coefficient for the system and can be used to calculate the temperature rise in the thermistor as a result of optical or electric power.

By multiplying the result from equation 2.8 with the voltage across the whole bridge will yield the output voltage. If the input voltage was 5 mV the output voltage would be: $1.62 \cdot 10^{-3} \cdot 5\mathrm{mV} =$

8.1μV. One could of course choose whatever voltage that is desirable but here 5 mV is sufficient to manifest the principle.

Assuming that the potentiometer is not perfectly balanced, e.g. 15kΩ on the R_d side and 10kΩ on the R_c side. Now the resistance values of these resistors will change to: $R_{d'} = 15\text{k}\Omega||1\text{k}\Omega = 0.9375\text{k}\Omega$ and $R_{c'} = 10\text{k}\Omega||1\text{k}\Omega = 0.9091\text{k}\Omega$. Assuming that R_a and R_b stays unchanged for now, the bridge is unbalanced. If R_a is changed with $\Delta\Omega = 1.8\Omega$ as before the result becomes slightly different:

$$\frac{\frac{R_b}{R_{d'}} - \frac{R_a - \Delta\Omega}{R_{c'}}}{(\frac{R_b}{R_{d'}} + 1)(\frac{R_a - \Delta\Omega}{R_{c'}} + 1)} = -0.8475 \cdot 10^{-3} \tag{2.10}$$

Again, assuming a $5mV$ input voltage gives

$$V_{\text{out}} = -0.8475 \cdot 10^{-3} \cdot 5\text{mV} = -4.2375\mu\text{V} \tag{2.11}$$

This result, or the previous, is subjected to amplification in the range of 100-10000.

One can adjust sensitivity by carefully choosing resistance values in the bridge. Increasing R_a and R_b will decrease the sensitivity, decreasing their resistance value will make the system more sensitive. If R_a or R_b act as sensor with a fixed sensitivity one can adjust R_c and R_d to obtain the same change in sensitivity.

2.5 Characterizing the Electric Setup

To characterize the circuit from figure 2.2 and identify how much current is flowing though the sensors the equivalent resistance must be found. If the total resistance is known one can calculate the amount of current in the circuit using $V = RI$. Examining figure 2.2 one can see that the 39kΩ resistor will dominate and almost on its own determine the current flow. The bridge circuit is in parallel with the 39Ω resistor which will decrease the resistance impact from the bridge.

$$R_{\text{eq}} = (((1\text{k}\Omega||6\text{k}\Omega) + 90\Omega)||39\Omega) + 39\text{k}\Omega = 39.03745763\text{k}\Omega \tag{2.12}$$

$$I = \frac{V}{R_{\text{eq}}} \tag{2.13}$$

Applying 5 V from the power supply one would get:

$$I = \frac{5\text{V}}{39.03745763\text{k}\Omega} = 128.08211\mu\text{A} \tag{2.14}$$

To work out how much current flows through the two bridge branches one can use the current division equation:

$$I_X = \frac{R_T}{R_T + R_X} \cdot I_T \tag{2.15}$$

where I_T and R_T is the total current and resistance. R_X is the resistance value of the desired branch where the unknown current, I_X, flows through. So $R_X = 39\Omega$, $I_T = I = 128.08211\mu\text{A}$ and $R_T = R_{\text{eq}} = ((1\text{k}\Omega||6\text{k}\Omega) + 90\Omega) = 947.143\Omega$ would give:

$$I_X = \frac{947.143\Omega}{947.143\Omega + 39\Omega} \cdot 128.08211\mu\text{A} = 123.0617158\mu\text{A} \tag{2.16}$$

Current flowing to the bridge will be:

$$I_b = I - I_X = 128.08211\mu\text{A} - 123.06171\mu\text{A} = 5.0204\mu\text{A} \tag{2.17}$$

And to each sensor:

$$I_{b1} = I_{b2} = 5.0204\mu\text{A}/2 = 2.5102\mu\text{A} \tag{2.18}$$

This can easily be adjusted by increasing the voltage or making some adjustments in the circuit like replacing the 39Ω with a larger resistor if one want more current to the sensors for instance.

If the current flows through the sensor in room temperature and the voltage drop across it would be

$$V_{\text{sensor}} = I_{b1} \cdot R_{\text{sensor}} = 2.5102\mu\text{A} \cdot 90\Omega = 225.918\mu\text{V} \tag{2.19}$$

225.918μV is not a large quantity and on the output it will be even lower since it is the voltage difference that is measured. The fact that the quantities are so small makes the system somewhat susceptible for noise.

2.6 The Diode And Thermal Design

The photodiode used is a Hamamatsu IR-photodiode of type S1337-66BR [10]. It is a silicon diode in a ceramic housing. It is suitable to measure and calibrate laser diodes. Ideally it would only be the silicon chip that made up the diode. With the ceramic housing it is more mass that needs to be heated by electric or optical power that just a low-mass silicon chip. With only the silicon chip the sensitivity would increase and less power is needed to make a temperature difference between the photodiode and the reference material.

Thermal design means, in this case, the way the two thermistors interact with the rest of the setup. The thermistors are individually attached to the reference copper plate and the photodiode respectively. But it is desirable that they are connected in such a way that they obtain the same temperature after a time period. To do this it must be established a heat link between them. The strength of this heat link decides how fast they obtain matching temperature. It is important that the heat link is not too strong because then it will influence the measurements. But it must not be too weak either, in this case thermal equilibrium between the sensors can not be achieved. One has to find a balance where the heat link is not too strong and not too weak. In this case a relative weak heat link is required because the reference should sustain a stable temperature during experiments. If this is not the case the results will be affected since the amplifier circuit amplifies the voltage difference between the two thermistors.

Figure 2.5 shows the first thermomechanical design. Figure 2.6 shows the final design. Inside the container is a the photodiode and the thermistors. There were other designs tried out, but they were soon replaced and therefore not featured in this report.

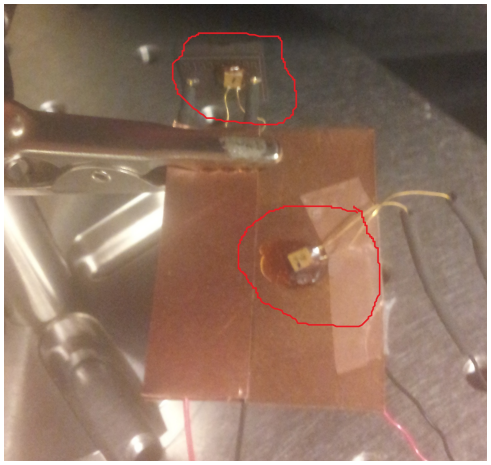

Figure 2.5: *The two red circles surrounds the two thermistors. The top red circle also includes the backside of the silicon photodiode. There are three sets of wires involved, one to the detector exiting the bottom part of the picture and two connected to the thermistors in the lower right hand corner.*

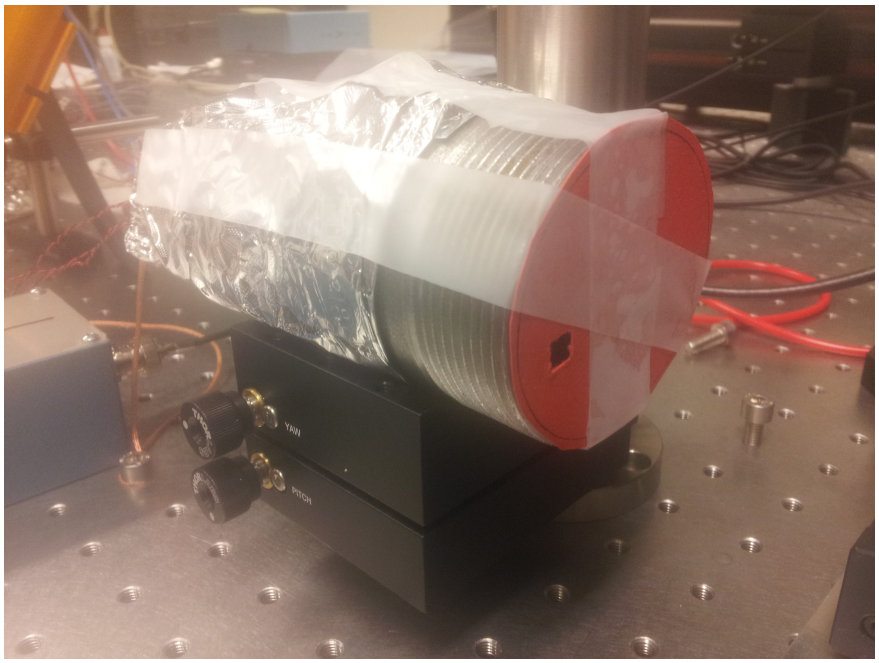

Figure 2.6: *In this container the photodiode and the two thermistors are shielded from possible noise sources. The hole on the left hand side on the front is to let the laser beam enter the system.*

The same principle of heat transfer between the thermistors are used in 2.5 and 2.6. The final setup has a screw and a custom made copper washer that connects the wires from the

photodiode to the reference material instead of a crocodile clip. The steel container is to protect the system from noise and temperature fluctuations. Added to the system was a second heat link connected from the reference copper plate to the optical laboratory table. The inside of figure 2.6 looks something like this:

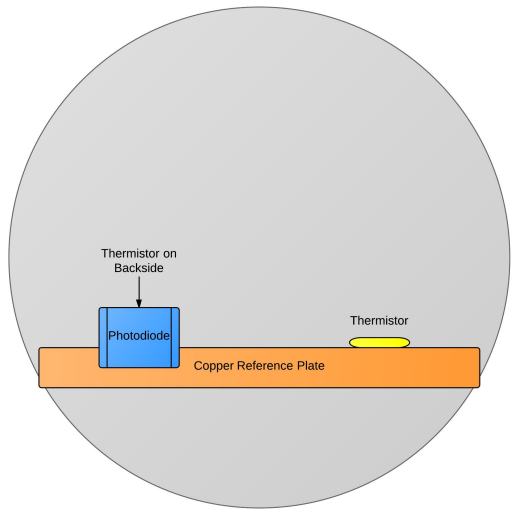

Figure 2.7: *The inside of the container. The wiring goes out on the backside of the container and the front is covered up with fitted cardboard.*

2.7 Reflection

The need to quantify reflection is important when calibrating optical power. Minimizing reflection from the surface will increase the accuracy of the system since reflections is calculated, not measured. By removing reflection losses from the equation one will have one less source of error to concentrate on. The calculation is based on a normal incident angle.

Reflections from a plane surface can be calculated using the Fresnel equations. To use these equations it is important to state some relationships between angles and refractive indicies that reflection and transmission on a planar surface has. The law of reflection states that the incident angle must be equal to the reflected angle from a planar surface:

$$\theta_i = \theta_r \tag{2.20}$$

Snell's law says that the angle of the transmitted ray depends on incident angle and the refractive indices of the two mediums that the light ray propagate between:

$$n_1 \sin\theta_1 = n_2 \sin\theta_2 \tag{2.21}$$

How the light ray behaves is also dependent on polarization. If the light is transverse electric (TE) polarized, i.e. the electric field is perpendicular to the plane of incidence, one get the following version of the Fresnel equations:

$$r_{TE} = \frac{n_1 \cos\theta_1 - n_2 \cos\theta_2}{n_1 \cos\theta_1 + n_2 \cos\theta_2} \tag{2.22}$$

Transverse magnetic (TM) polarization, i.e. the magnetic field is perpendicular to the plane of incidence, gives:

$$r_{TM} = \frac{n_1 cos\theta_2 - n_2 cos\theta_1}{n_1 cos\theta_2 + n_2 cos\theta_1} \tag{2.23}$$

Derivation of the Fresnel equations can be found here [19].

2.7.1 Calculation of Reflection Coefficient

Now that the framework is presented one can calculate how much of the incident light is reflected from the surface of the photodiode. From [9] one can obtain the refractive index of intrinsic silicon at 300 K. The laser wavelength is 488 nm which gives a refractive index $n_{Si} = 4.419$ and an extinction coefficient $k_{Si} = 0.055$. The extinction coefficient describes how radiation is absorbed in a medium. The absorption coefficient is given by $\alpha = 4\pi k/\lambda$. A thin layer of SiO_2 is on top of the silicon substrate. The refractive index of SiO_2 at 488 nm is $n_{SiO_2} = 1.54953$ [6]. The oxide thickness of the Hamamatsu s1337 is 29 nm [8]. Reflections will occur at the interface of air-SiO_2 and SiO_2-silicon substrate. To calculate the reflection one can use the Fabry-Perot etalon as a model [12].

When dealing with a normal incident angle, i.e. $\theta_i = 0°$, the Fresnel equation can be simplified. Given a normal incident angle gives:

$$r_{TE} = \frac{n_1 - n_2}{n_1 + n_2} = r_{TM} \tag{2.24}$$

The transmission coefficient becomes:

$$t = \frac{2n_1}{n_1 + n_2} \tag{2.25}$$

r_{TE}, r_{TM} and t are amplitude coefficients. Convert them into power coefficients:

$$R = |r|^2 \tag{2.26}$$

$$T = \frac{n_2}{n_1}|t|^2 \tag{2.27}$$

Conservation of energy gives:

$$R + T = 1 \tag{2.28}$$

For completely unpolarized light the total reflected power is:

$$R = \frac{|r_{TE}|^2 + |r_{TM}|^2}{2} \tag{2.29}$$

The laser beam is unpolarized, i.e. the reflection coefficients for TE and TM are equal and equations 2.24 and 2.26 can be used to obtain the power reflected.

One can view the air, silicon dioxide and silicon layers as a Fabry-Perot etalon. To calculate the reflection coefficient of unpolarized light:

$$r = r_{12} + \frac{t_{12}t_{21}r_{23}e^{-2i\delta}}{1 - r_{21}r_{23}e^{-2i\delta}} \tag{2.30}$$

where r and t represents the reflection and transmission coefficients between the different layers and 1,2,3 represents air, silicon dioxide and silicon respectively. $\delta = 2\pi d n_{SiO2}/\lambda$ where d is oxide thickness and λ is the wavelength of the light. Derivation of the respective reflection and transmission coefficients in a Fabry-Perot environment can be found here [19]. Using the information about oxide thickness, refractive index of SiO_2 and the laser wavelength gives $\delta = 0.578573$. Using equations 2.24, 2.25 and 2.26 gives total reflected power:

$$R = 0.3299 \tag{2.31}$$

R gives the fraction of the incident power being reflected from the surface of the photodiode. If a 5 mW laser beam was to hit the photodiode with an normal angle of incidence, the power reflected would be:

$$5\text{mW} \cdot 0.3299 = 1.6494\text{mW} \tag{2.32}$$

2.7.2 Minimizing Reflection Loss

There are many ways to minimize optical losses that can occur on a surface. Parallels can be draw to the solar cell industry where much effort is put in to capture as much sunlight as possible. Anti-reflex coating, texturing of the surface and increased cell thickness to reduce backside reflection are some of the measures that the solar industry use. Other methods involve mirrors and other optical elements.

One could imagine a trap configuration, like presented here [17], that generates m internal reflections so $R_{\text{new}} = R^m$.

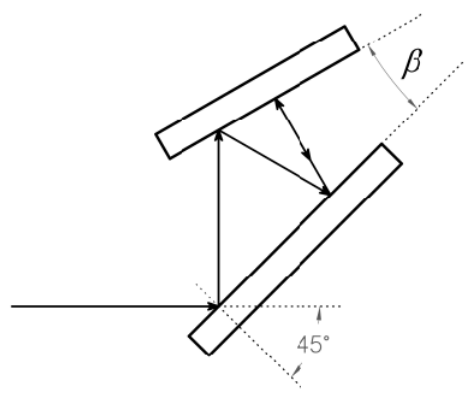

Figure 2.8: *Demonstrates the principle of a trap configuration. By changing β and incident angle one can determine the number of reflections [17].*

By installing a highly reflective mirror as one of the elements in figure 2.8 and the photodiode as the other one can increase the number of internal reflections, thus reducing reflection loss. Obviously, the incident angle would change for each internal reflection but they can be calculated using simple geometry and one would get $R = R_{\theta 1} R_{\theta 2} R_{\theta 3} R_{\theta 4} \cdots R_{\theta m}$, where θ_m represents

the incident angle of each internal reflection.

2.8 Noise Analysis

In this chapter possible noise sources are identified and analysed. The setup is very sensitive for noise so it is important to minimize the noise effect.
Noise is often measured using spectral density. It is noise voltage or current per root hertz, i.e. $\frac{\mathrm{V}}{\sqrt{\mathrm{Hz}}}$ or $\frac{\mathrm{A}}{\sqrt{\mathrm{Hz}}}$. This is because the characteristic equations that identify noise are integrated over frequency, indicating that spectral density is the natural way to express noise sources [11].

2.8.1 Types of Noise

In electronic circuits there are five common noise sources:

- Shot Noise
- Thermal Noise
- Flicker Noise
- Burst Noise
- Avalanche Noise

In op amp circuits designs, like the instrumentation amplifier, burst and avalanche noise are normally not an issue.

Shot Noise

Shot noise is spectrally flat, temperature independent and occurs when a charge crosses a potential barrier. This means that shot noise occurs with current flow through a potential gap. The event that a charged particle pass a potential barrier is purely random. The current created is composed of many random, independent current events. Shot noise does not occur in conductors or resistors.

Thermal Noise

Thermal noise is caused by a change in temperature in passive resistive elements. This type of noise is spectrally flat and is independent of current flow. Thermal noise can be modelled as both voltage and current. A voltage source in series with a noiseless resistor can model voltage noise. To model current noise a current source in parallel with a noiseless resistor is used.

$$e_R = \sqrt{4kTR_{eq}\Delta f} \tag{2.33}$$

where e_R is the noise in V, k is Boltzmann's constant, T is absolute temperature and R_{eq} is equivalent resistance in the circuit. Δf is the bandwidth of the system. Thermal noise is white noise, i.e. equal power density for all frequencies.

Flicker Noise

Flicker noise is often known as $\frac{1}{f}$ noise. It exists in all active electronic devices and is associated with DC current because it is resistance fluctuation, which can be related to voltage or current fluctuation through Ohm's law. Flicker noise can is often a problem at low frequencies because it tends towards infinity when integrating around DC. At higher frequencies other types of noise dominates.

Burst Noise

Burst noise is caused by imperfections in semiconductor material and heavy ion implants. It occurs when charge carriers are randomly trapped or released at interfaces or in crystal defects.

Avalanche Noise

Avalanche noise occurs when a pn junction is operated in the reverse breakdown mode. What happens is that charge carriers in a high voltage gradient has enough energy to tear off other charge carriers through physical contact creating random current pulses.

2.8.2 Instrumentation Amplifier Noise

The noise in an instrumentation amplifier with high gain comes predominantly from input noise. All noise on the amplifiers input will be amplified together with the differential signal. When analysing noise in an instrumentation amplifier it is common to model it with one or two stages; input and output stage. Voltage noise sources are are placed at the input and at the output (V_{n_in} and V_{n_out}). V_{n_RTO} represents the noise referred-to-the-output (RTO). The total noise can be expresses as the root sum of squares of input and output noise.

$$V_{n\_\text{RTO}} = \sqrt{(V_{n\_\text{out}})^2 + (V_{n\_\text{in}} \cdot G)^2} \tag{2.34}$$

By dividing V_{n_RTO} with the gain the noise referred to the input (RTI) can be obtained.

$$V_{n\_\text{RTI}} = \sqrt{(\frac{V_{n\_\text{out}}}{G})^2 + (V_{n\_\text{in}})^2} \tag{2.35}$$

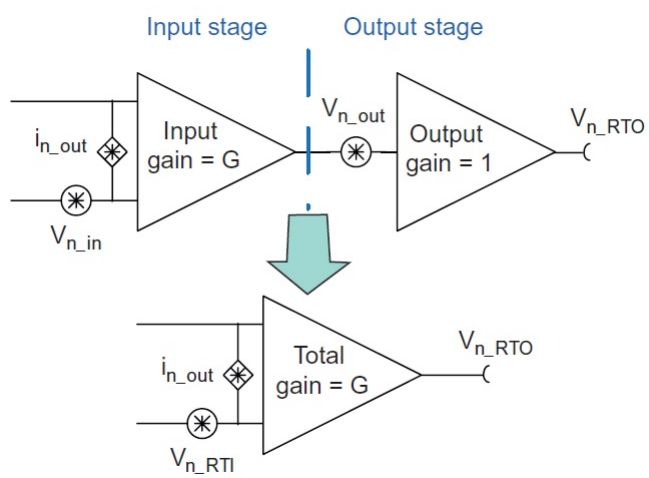

Figure 2.9: *Noise model for one or two stages [13].*

It is a common misconception that the gain does not affect the noise. In fact, the noise at the input will be amplified as much as the desired input signal. A low-pass filter at the instrumentation amplifier inputs could prevent high frequencies from reaching the instrumentation amplifier.

2.8.3 Noise Calculations For The Setup

According the data sheet [3] the AD620 instrumentation amplifier has the following specifications for noise:

Table 2.1: *Noise specifications from the AD620 data sheet [3].*

Parameter	Min	Typ	Max	Unit
Input Voltage Noise	-	9	13	$\frac{\text{nV}}{\sqrt{\text{Hz}}}$
Output Voltage Noise	-	72	100	$\frac{\text{nV}}{\sqrt{\text{Hz}}}$
RTI, 0.1 Hz to 10 Hz				
G = 1		3.0		μV p-p
G = 10		0.55		μV p-p
G = 100-1000		0.28		μV p-p
Current Noise at f=1 kHz		100		$\frac{\text{fA}}{\sqrt{\text{Hz}}}$
0.1 to 10 Hz		10		pA p-p

It is necessary to know the equivalent input resistance in order to obtain knowledge about the thermal noise from the resistors. From section 2.5 we get that $R_e q = 39k\Omega$

$$e_R = \sqrt{4 \cdot 1.38 \cdot 10^{-23}\text{JK}^{-1} \cdot 297\text{K} \cdot 39\text{k}\Omega} = 25.3\text{nV}/\sqrt{\text{Hz}} \tag{2.36}$$

This noise calculation applies for the added resistors in the circuit which represents thermal noise. Assuming that the current noise, i_n, on the positive and negative input of the instrumentation amplifier is equal ($|i_{np}| = |i_{nn}|$), the equation becomes:

$$e_{in} = \sqrt{(i_{np} \cdot R_{\text{eq}})^2 + e_{Rp}^2 + (i_{nn} \cdot R_{\text{eq}})^2 + e_{Rn}^2} \tag{2.37}$$

The thermal noise on the resistors are the same for the positive and the negative input ($e_{Rp} = e_{Rn}$).

$$e_{in} = \sqrt{2 \cdot (i_n \cdot R_{\text{eq}})^2 + 2 \cdot e_R^2} \tag{2.38}$$

The current noise value is obtained from the AD620 data sheet [3] and is also found in table 2.1.

$$e_{in} = \sqrt{2 \cdot \left(100 \frac{\text{fA}}{\sqrt{\text{Hz}}} \cdot 39\text{k}\Omega\right)^2 + 2 \cdot \left(25.3 \frac{\text{nV}}{\sqrt{\text{Hz}}}\right)^2} = 36.2 \frac{\text{nV}}{\sqrt{\text{Hz}}} \tag{2.39}$$

Equation 2.39 is the total amount of thermal noise in the external bridge circuit. To find the total noise in the system all of the noise sources must be taken into account. Those are input and output noise of the instrumentation amplifier together with the thermal noise calculated in equation 2.39. Let the gain be set to 200.

$$e_{tot} = \sqrt{\text{Input Noise}^2 + \left(\frac{\text{Output Noise}}{\text{Gain}}\right)^2 + \text{Thermal Noise}^2} \tag{2.40}$$

$$e_{tot} = \sqrt{\left(13 \frac{\text{nV}}{\sqrt{\text{Hz}}}\right)^2 + \left(\frac{100 \frac{\text{nV}}{\sqrt{\text{Hz}}}}{200}\right)^2 + \left(36.2 \frac{\text{nV}}{\sqrt{\text{Hz}}}\right)^2} = 38.5 \frac{\text{nV}}{\sqrt{\text{Hz}}} \tag{2.41}$$

Theoretically the noise in the instrumentation amplifier should not exceed $38.5 \frac{\text{nV}}{\sqrt{\text{Hz}}}$.

Chapter 3

Characterization of the System

When characterizing the system it is desired to identify the properties of the system. I.e. what does the system give as an output given a certain input type. What affects the system? Is it linear? Is it predictable? Is it time-invariant? These are some the questions that will be provided with an answer in this chapter. Firstly, some of the expectations of the system will be reviewed.

3.1 Expectations

It is expected that the system will act linearly and time-invariant. It is also expected that the system will yield the same result for a given input, i.e. that the system is deterministic. Expected issues are predominantly noise issues. Measures to reduce noise will be presented in section 4.1.

3.2 Characterization of the System

The characterization of the system can be divided into two parts.

(i) A series of electric power measurements are done to create a table that will act as a simple tool when approximating electric power to match the optical power. To identify the voltage difference generated by the electric power accurately one can use the curve fitting tool in Matlab. It is expected that each pulse will be on the form $a \cdot \left(1 - e^{\frac{-t}{b}}\right)$, where a is the voltage difference

generated, t is the time and b is the time constant of the pulse. Each pulse generates a separate voltage difference,a, and it is these values that are used to create the table. When measuring an unknown optical power it generates a voltage difference. The idea with the table is that one can approximate the electric power needed by identifying the applied power that corresponds to the voltage difference generated by the unknown optical power.

(ii) Measure the voltage difference that the laser generates and, with the aid of the table, perform two electric power measurements; one slightly above the voltage difference generated by the incident laser beam and one slightly below the voltage difference generated by the incident laser beam. For every optical calibration this step must be performed. The table needs only to be generated one time as it only works as a tool during the calibration.

3.2.1 Electric Power Measurements to Generate Table

Several thermal design were tested, the first one had a thin and low-mass reference plate shown in figure 2.5. By increasing the thermal mass and creating a more robust setup the first prototype was made (figure 2.6). The measurements were performed at the optics lab at Justervesenet.

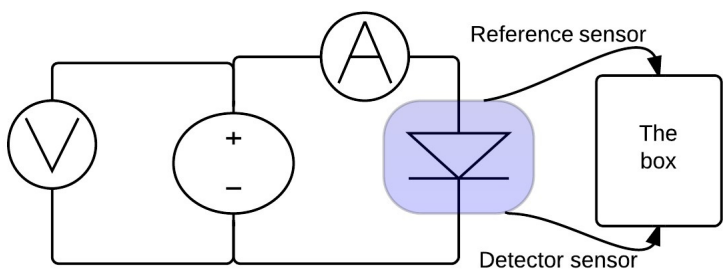

Figure 3.1: *Voltage was applied and current and voltage were measured with a voltmeter and ammeter. The blue section represents the thermomechanical design. The box detects the voltage difference between the sensors and amplifies it. The result is read from the box output.*

The electric measurements were done with the use of electric current to heat the photodiode and measure the response. By an ammeter in series and a voltmeter in parallel, like figure 3.1 shows, it is trivial to find the power deposited, through $P = IV$.

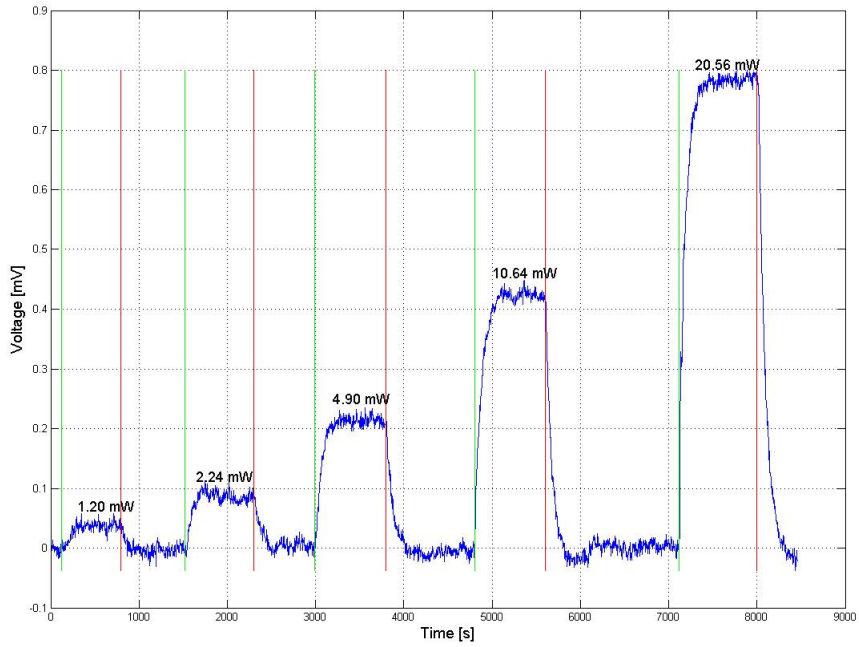

Figure 3.2: *Calibration using electric current to heat the photodiode. The number of each pulse represents the calculated power generated by the power supply. The green and red vertical lines represents the time when the voltage was applied and turned off respectively.*

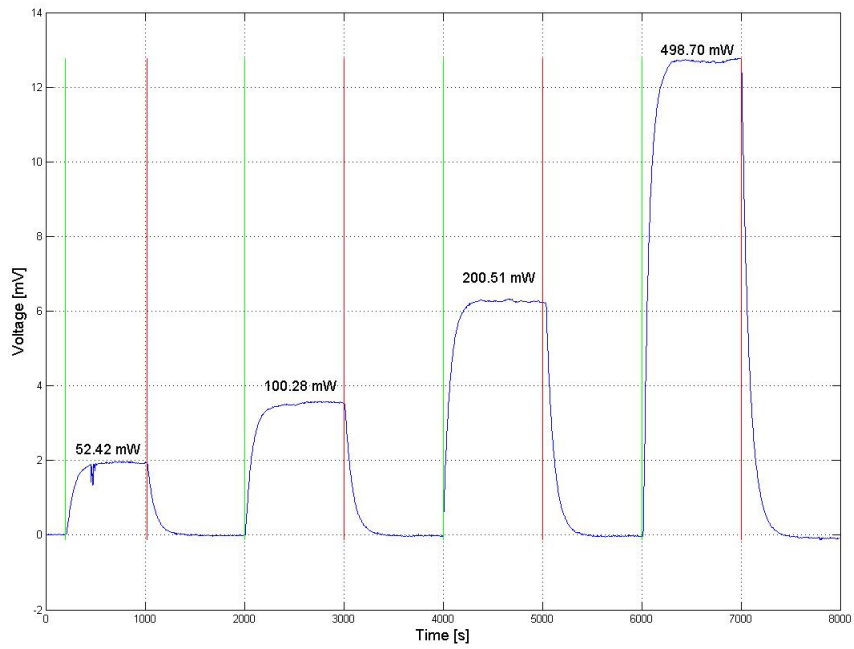

Figure 3.3: *Calibration using electric current to heat the photodiode. The number of each pulse represents the calculated power generated by the power supply. The green and red vertical lines represents the time when the voltage was applied and turned off respectively. The dip in the first pulse is an obvious error and not is considered when fitting a curve to the pulse.*

The results from these electric measurements were used to generate a table that would be the basis of comparison when calibrating the optical power. To do this each power pulse were fitted a curve using the curve fitting tool in Matlab. By making use of the rising flank of each pulse and generating two vectors from the raw data, time and voltage difference, one can simply use the two vectors as inputs in the curve fitting tool which will generate a fitted curve. One could also take the average of the last half of each pulse to generate a value to be used in a table. The results of the curve fitting can be found in appendix A. From the curve fitting in Matlab different time constants where obtained. The average time constant over nine pulses was 66.492 seconds. The curve fitting provided values for the voltage difference generated by the electric power. Plotting the voltage difference and the corresponding electric power would give an indication of the linearity of the system. Such a plot can be found in figure 3.4.

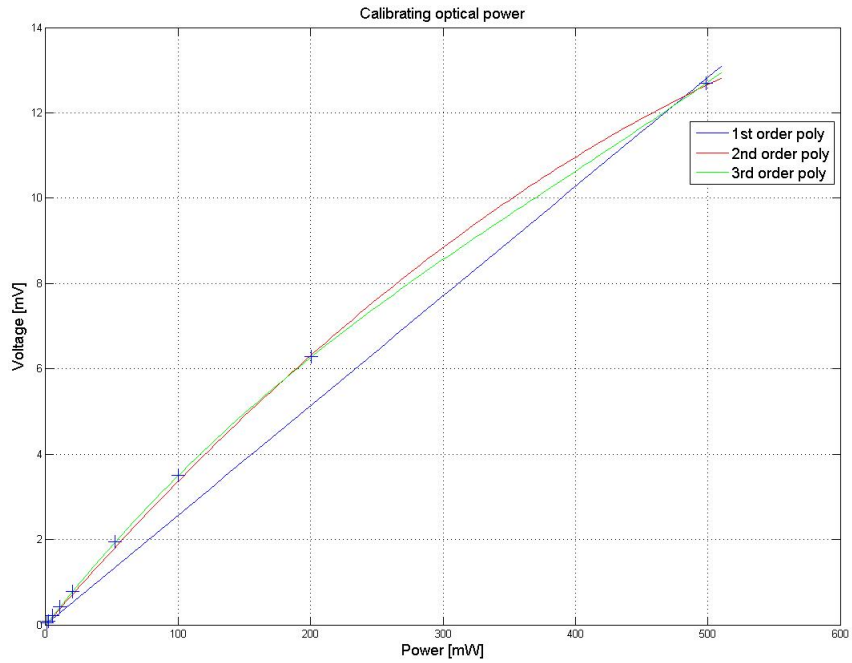

Figure 3.4: *The results from the electric power measurements. Using the data points to generate graphs that fitted with the data were done. First, second and third order polynomials were generated using the curve fitting tool in Matlab that fit the data points best. The crosses represents the voltage difference generated by the electric power, i.e. the data points.*

Figure 3.4 shows the results of the electric power measurements. The third order polynomial has the best fit, but it is unknown how it behaves on higher powers so that is discarded. It is more probable that the first or second order polynomial would be more realistic when considering higher powers. More measurements on higher powers are needed to characterize the system satisfactory. The equations for these two curves can also be used a tool when calibrating above and below the voltage difference generated by the laser. The first order equation looks like this:

$$\Delta\text{voltage} = \text{power} \cdot 0.02568 \qquad \text{mV} \tag{3.1a}$$

$$\text{power} = \frac{\Delta\text{voltage}}{0.02568} \qquad \text{mW} \tag{3.1b}$$

For the second order polynomial one must solve the quadratic equation as if c=-voltage in order to fulfil $ax^2 + bx + c = 0$:

$$\Delta\text{voltage} = -2.074 \cdot 10^{-5} \cdot \text{power}^2 + 0.03569 \cdot \text{power} \qquad \text{mV} \tag{3.2}$$

$$\text{power} = \frac{-0.03569 \pm \sqrt{0.03569^2 - 4 \cdot (-2.074 \cdot 10^{-5}) \cdot (-\Delta\text{voltage})}}{2 \cdot (-2.074 \cdot 10^{-5})} \qquad \text{mW} \tag{3.3}$$

The quadratic equation yields obviously two solutions. The solution that is interesting is the one within the interval set by the upper and lower limits of the electric calibration which will be presented in the next section. One can insert the voltage difference obtained from the optical voltage measurement in equation 3.3 and get a calibrated power value this way. But the main idea is to do measure the voltage difference generated by the laser and then calibrate with two electric measurements, one slightly above and one slightly under the the voltage difference obtained by the optical voltage measurement. To identify how much power to apply when calibrating electrically one can use a table with that fits figure 3.4.

Table 3.1: *The table shows voltage difference values with corresponding power values. The table act as a tool when calibrating above and below the voltage difference generated by the optical power. The table is not adjusted for reflection losses.*

Δvoltage	**Power**
0.03856 mV	1.2 mW
0.08661 mV	2.24 mW
0.2148 mV	4.9 mW
0.4257 mV	10.64 mW
0.7843 mV	20.56 mW
1.945 mV	52.42 mW
3.505 mV	100.28 mW
6.28 mV	200.51 mW
12.70 mV	498.7 mW

3.2.2 Calibrating Optical Power

When the table is established one can do two electric power measurements to calibrate the optical power. But first, one must measure the voltage difference generated by the laser and use the

curve fitting tool in Matlab to obtain a Δvoltage value that will be the basis of calibration (figure 3.5). To act as an optical power source a Kr^+ laser from *Coherent* was used with wavelength 488 nm. A laser stabilizer was used to keep the laser power as constant as possible.

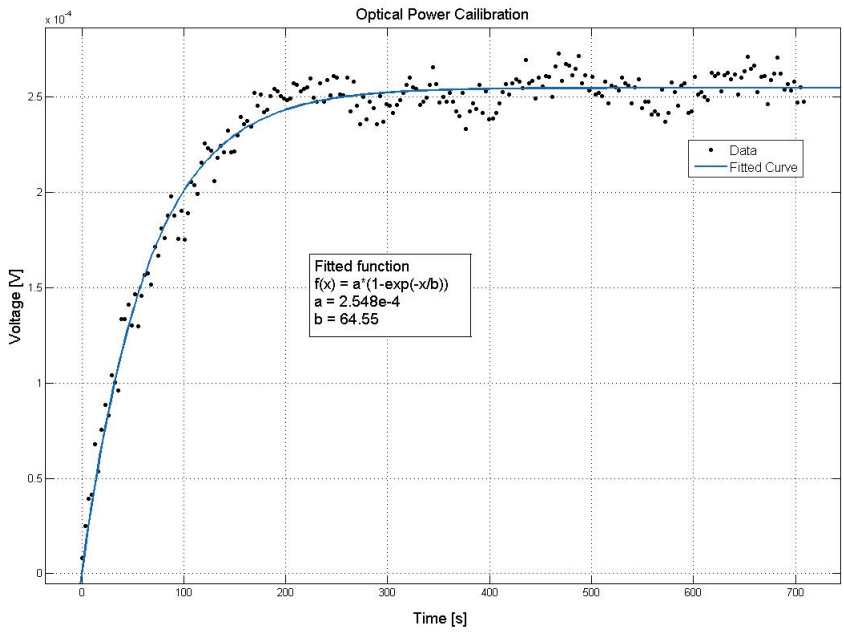

Figure 3.5: *Curve fitted to the voltage difference generated by the optical power source as a function of time.*

Using table 3.1 or equation 3.3 one can approximate how much electric power is needed to place one curve above and one below the voltage difference generated by the optical power source. Using table 3.1 the calibration above was done with 7.67 mW and the one slightly below was done with 4.93 mW. Both calibrations were curve fitted as well and are shown in figures 3.6 and 3.7.

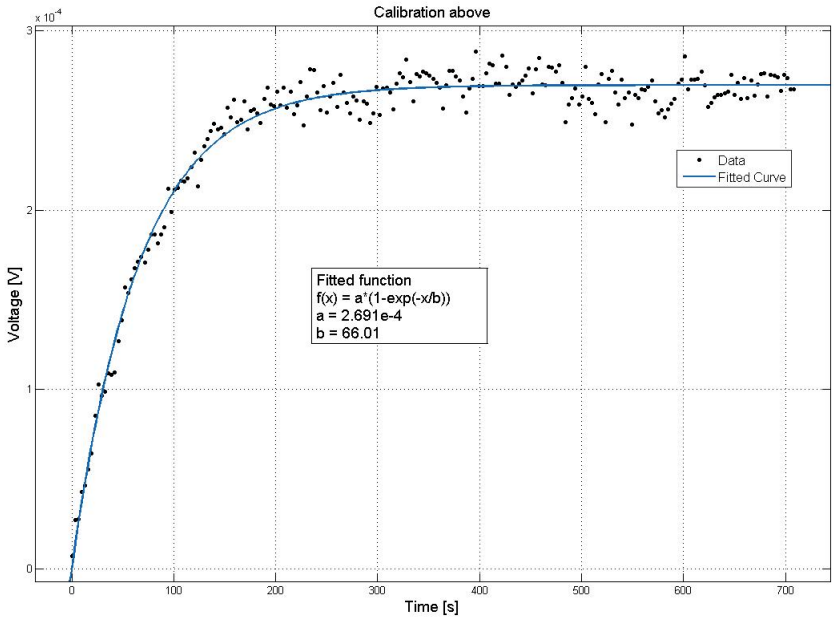

Figure 3.6: *Curve fitted to the calibration above the voltage difference generated by the optical power source. The power applied was 7.67 mW.*

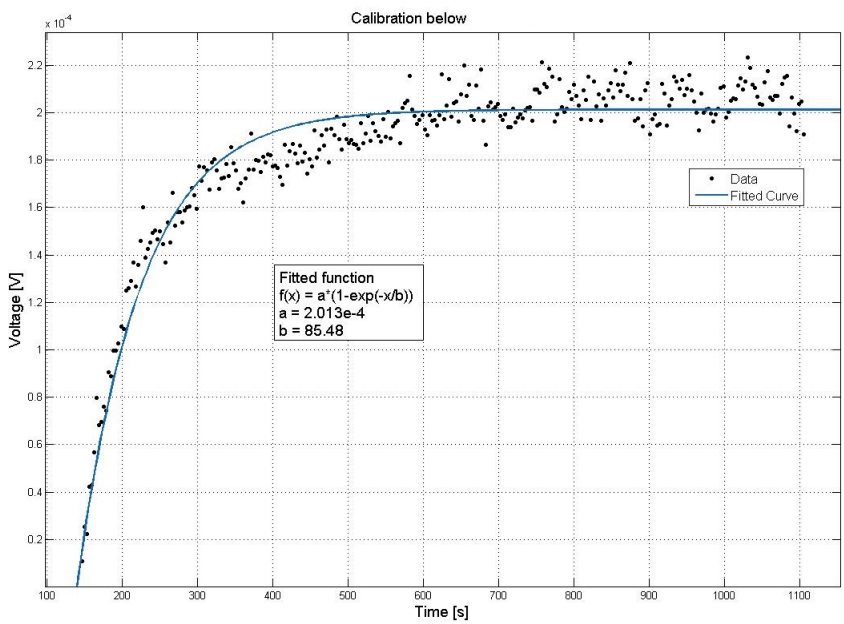

Figure 3.7: *Curve fitted to the calibration below the voltage difference generated by the optical power source. The power applied was 4.93 mW.*

The three fitted curves can be plotted in one graph, to see how close the electric calibrations are to the optical one. This is the basis for the calibration. The next step is to calculate the power that corresponds to the voltage difference generated by the laser beam.

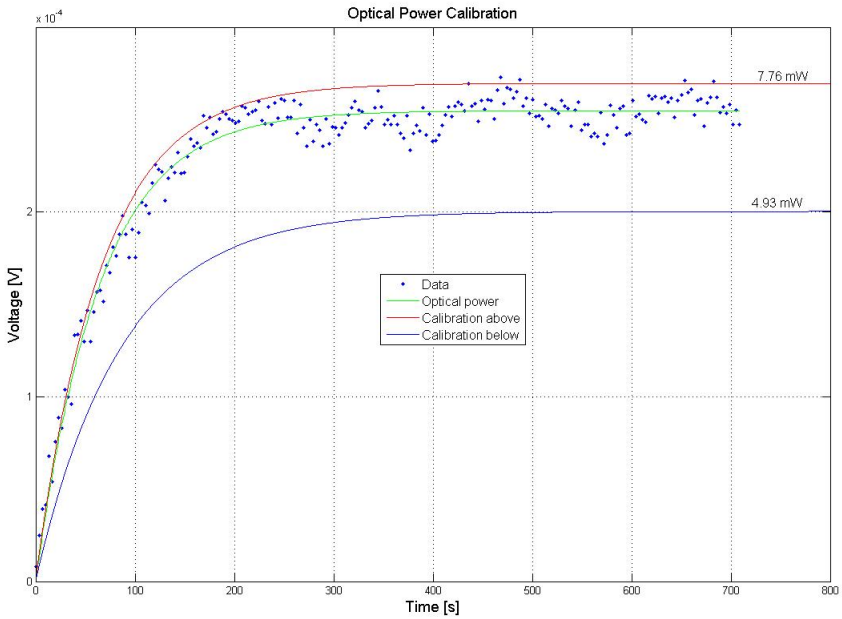

Figure 3.8: *The results from the optical calibration. One above and one under the optical power. The dots are data points used for the curve fitting. The power values in the figure represents the power applied to generate the voltage difference.*

From figure 3.8 one can deduct the interval in which the optical power lies within, [4.93 mW 7.67 mW]. Utilizing the saturation values from the curve fitting process as Δvoltage for each graph and assuming that the graph is linear within the interval one can obtain the optical power:

$$P_a = 7.67\text{mW}, \qquad V_a = 0.2691\text{mV} \tag{3.4a}$$

$$P_b = 4.93\text{mW}, \qquad V_b = 0.2013\text{mV} \tag{3.4b}$$

$$P_o = \text{unknown}, \qquad V_o = 0.2548\text{mV} \tag{3.4c}$$

where P_a, P_b and P_o represents the power of the calibration above, calibration below and optical respectively. The same is applicable for V_a, V_b and V_o. It is necessary to know where within the

interval P_o lies. Assuming a that the optical power (P_o) has the same relative distance from P_a as V_o has to V_a.

$$P_a - P_b = 2.74 \tag{3.5}$$

$$V_a - V_b = 0.678\text{mV} \tag{3.6}$$

$$V_a - V_o = 0.143\text{mV} \tag{3.7}$$

$$d_{rel} = \frac{V_a - V_o}{V_a - V_b} = 0.2109 \tag{3.8}$$

$$P_{rel} = d_{rel} \cdot (P_a - P_b) = 0.5779\text{mW} \tag{3.9}$$

This means that the optical power, P_o, is:

$$P_o = P_a - P_{rel} = 7.0921\text{mW} \tag{3.10}$$

Adjusting for reflective losses from the surface the calibrated optical power becomes:

$$P = P_o/(1 - R) = 10.5836\text{mW} \tag{3.11}$$

where R is the reflected power calculated in section 2.7.1.

3.3 Sources of Error

It is unknown how stable the system is, due to the lack of testing of the final setup. Does the electric current cause the same rise in temperature in the photodiode every time given a fixed input power? To properly characterize the system and to identify the uncertainties it is necessary with several measurements with as equal input variables and conditions as possible. This is valid for both the electric and optical measurements. From figures 3.6, 3.7, 3.5 and the figures in appendix A one can see that the time constants are not the same. Ideally they should be equal, especially for the electric calibrations. The reason for this could be noise or some sort of thermal drift in the system.

When using electric current to heat the photodiode it is not given that 100% of the power generated by the power supply will go towards heating. Some of the power will disappear as

heat in wires and contacts.

Noise remains the biggest challenge which could arise from grounding issues in the electric setup. To produce a positive and negative voltage to supply the instrument amplifier two power supplies in series are used. This gives no power ground, only signal ground.

Other sources of error that could affect the electric setup is the wiring. Most of the wires are twisted to reduce the chance of picking up any unwanted signals. But the wires could still pick up some noise and the fact that the input signal to the instrumentation amplifier is small (μV) makes the noise more influential. All the wires from the thermomechanic setup should ideally be merged and twisted into one wire to further reduce noise. The same thing could apply for the wiring from the box that contains the electric circuit. Noise from the instrumentation amplifier has been discussed but it should not be ignored as a possible noise source.

The reflection losses are based on a normal incident angle but there may be some deviation from this angle in the actual measurement. The reflection losses could be somewhat larger than calculated if the photodiode surface is not perfectly normal with respect to the incident laser beam.

The measurement equipment on the lab are accurate, a custom made program has been made for similar purposes. One could make the measurements even more accurate by averaging over a number of measurements to create one data point. Suggestions for improvement of the system will be presented in more detail in section 5.1.

Figure 3.1 shows that the voltmeter has not got the optimal placement. It should be measuring the voltage across the photodiode, not the total voltage supplied. This means that some power will be deposited in the ammeter, which will offset the results.

Chapter 4

Discussion

In this chapter discussions around the work process and results are discussed.

4.1 Noise Reduction

In the beginning of the process the system, and in particular the box, was noisy.

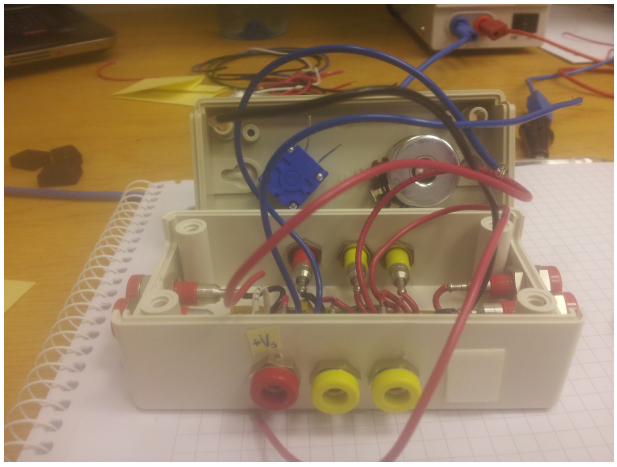

Figure 4.1: *A picture of the first electric setup contained in a plastic box.*

The first measure taken was to replace the plastic box with an aluminium box for more protection. That was helpful because it provided more space than the plastic box which made it easier to make electronic adjustments within the circuit. But it did not make any noticeable difference when it came to reducing noise. What did make a difference however, was to replace

the variable resistor that adjusted the gain, R_g, with a fixed resistor. This was done together with installing capacitors at the positive and negative power supply inputs at the instrumentation amplifier. Also low pass filters at the positive and negative inputs were installed. This, together with a separate low pass filter at the output of the box, reduced the noise. The primary noise source was probably the potentiometer used to set the gain. With that in mind the second potentiometer, used to balance to bridge, was replaced. A set resistor and a discrete variable resistor were put in its place as figure 2.2 shows. Figure 4.2 shows the box in its final state.

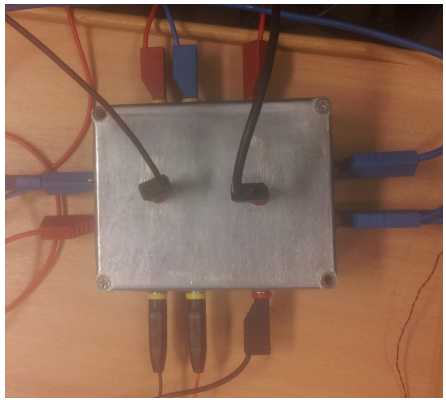

Figure 4.2: *A picture of the aluminium box that contains the electric setup.*

It was still somewhat noisy but noise generated from the thermal design could be reduced by changing the design. At first the copper plate was small, low mass and fasten to the optical laboratory table. A problem with this design was that the thermistor was susceptible to air gusts that could generate temperature fluctuations. The same thing could happen to the thermistor glued on the backside of the photodiode. There was not any heat link between them which meant a temperature difference between them would always be present, but this could be counterbalanced by adjusting the discrete variable resistor. Before the mass of the copper plate was increased a weak heat link was introduced. This would cause a weak heat exchange between the two objects involved; the reference copper plate and the photodiode. The idea behind this measure was to try to force the two objects to the same temperature. The advantage with this is that the voltage difference would be naturally balanced and made the thermistors less susceptible to noise. This is a good idea if the mass of the reference copper plate is sufficiently large enough so that it will not be affected by the temperature change in the photodiode

via the heat link. Increasing the mass of the reference copper plate will demand more energy to change the temperature. The final solution for the thermomechanical design is shown in figure 2.6 and 2.7. Putting everything in an almost sealed steel container provided protection from air gusts that potentially could influence the thermistors resistance value. It also becomes more robust to physical movement and knocks. Covering up the front was, in addition to protection from air gusts, meant to shield the photodiode as much as possible from light from the local environment. A sudden flash of light or a stable flow of light incident on the photodiode could cause inaccuracy or offsets in the measurements. The measurement instrument, Keithley 2000 M [14], on the lab has the possibility to take the average over several data points. This could be an useful tool when reducing noise.

4.2 Calibrating Optical Power

The advantage with this system is that it can handle a wide range of optical powers in room temperature. The limitation is set by the photodiode which tolerates currents up to 500 mA. The amount of power one get out of 500 mA is determined by the IV-curve of the photodiode. If larger powers are requested the current photodiode is easily replaceable by a more tolerant photodiode. One could buy a new one with improved current toleration or one could strengthen the wiring in the photodiode. For very low powers the system tends to drown in noise and becomes very inaccurate. The 1 mW pulse from figure 3.2 demonstrates this.

Another problem that has not bee discussed yet is the cool down process. One could experience that the system cools down to different voltage values, i.e. seemingly different temperatures. There could be a thermal drift present which again would affect the next measurement. Even though such an offsets is small, around 0.02 mV, it does affect the system and must be considered. The offset may also arise from noise.

Other things that could influence the measurement is that all the electric power may not contribute in a rise in temperature in the photodiode. Some losses must be assumed in wires and soldering contacts. Instead of using the rising flank of the pulse one could use the falling flank. In theory this would not make any difference.

It remains to be seen how deterministic the system is. More measurements are needed to

calculate uncertainties. The same test has to be done several times to obtain enough data. An instability in the system may be caused from the photodiode or the electric setup. If a given input yields very different output one would have to review the system closely. A suggestion that more measurements are needed comes from the two 4.9 mW calibrations, the first comes from making table 3.4 and the second comes from the calibration below the voltage difference generated by the optical power source (figure 3.7). Both has approximately the same input power but have a discrepancy in voltage difference. Between the two measurements there is a difference of 0.0135 mV. However, this deviation from equality could be caused by noise or some offset from thermal equilibrium. Uncertainties in the curve fitting tool in Matlab can also be a source of error. Other preferences in the curve fitting tool could give more precise results.

A different way of calibrating optical power with one electric calibration could be done by adjusting the input power to the optical power, immediately after the laser shutter closes. Then compensating for the decrease in temperature in the photodiode by heating the photodiode electrically and maintaining the same voltage difference. The electric power used to maintain this voltage difference would then be equal to the optical power. This is the standard way of doing it according to the theory concerning ESR. This process could be made automatic by introducing a custom made program that does the curve fitting as the measurement progresses. Then one can create another program that controls the power supply and using a numerical method to adjust the electric power to fit the voltage difference generated by the optical power.

Linearity is obviously a desired property in the system but it is not quite linear as figure 3.4 shows. Linearity here means that if one was to double the input power the voltage difference would also be doubled. By comparing the ratios of power and voltage difference for each pulse from table 3.1 one can see that linearity is not present in the current system. Ideally they would have the same ratio, e.g. $P_{20\text{mW}}/\Delta V_{20\text{mW}} = P_{50\text{mW}}/\Delta V_{50\text{mW}}$. Examining the results from table 3.1 one obtains the following ratios:

Table 4.1: *Table of ratios.*

Power	$\frac{\textbf{Power}}{\Delta V}$
1.2 mW	31.12
2.24 mW	25.86
4.9 mW	22.81
10.64 mW	24.99
20.56 mW	26.21
52.42 mW	26.96
100.28 mW	28.6
200.51 mW	31.9
498.7 mW	39.27

From table 4.2 one can see a tendency of increasing ratios from the $4.9mW$ pulse and on. This is of course a result of the quadratic nature of the function from figure 3.4. The first two points in the table does not fit with the tendency of the rest of the table points. This deviation from the tendency could arise from the incorrect position of the voltmeter in figure 3.1. The first two pulses has a low input power and noise will be more dominant at low powers so that could also explain the deviation from the rest of the measurements.

An important question that comes up is; how accurate is the system? The accuracy and sensitivity is important. One way to increase the sensitivity is to replace the photodiode with a pure silicon chip. With no ceramic housing and less mass to heat the system will become more sensitive and accurate if this solution was to be implemented. The accuracy depends on how precise one can measure voltage and current when using electric power. Here regular multimeters has been used. They can measure DC voltage down to $100\mu V$ and DC current down to 1μA. But since the photodiode needs around 0.5 V applied to allow current to flow the resolution is limited. Using other measurement equipment to measure voltage and current more precisely would increase accuracy. Assuming the voltage difference generated by the optical and electric power are correct and the curve fitting is accurate one can calibrate optical power very precise, down to 10^{-7} W.

4.3 Use

Advantages with the system is that it is applicable for calibration of high and low optical powers and the fact that it is used in room temperature. Most ESR today use cryogenic temperatures. The electric design is relatively simple and inexpensive. The termomechaical design can be installed in many variations to fit most applications. The system can be used to calibrate any optical power source over a wide spectral area. Since the system converts temperature rise into optical power the limiting spectral factor is the reflectance. Reflectance from the photodiode surface is spectrally dependent but by introducing a trap configuration, as presented in section 2.7.2, one generates a spectrally independent system. The temperature sensor circuit can also be applicable in other systems like temperature monitoring.

Parts of the system and the basic principle will also be used in an ongoing Ph.D. project where the fundamental constants e and h are going to be measured very precisely.

Chapter 5

Conclusion

The system calibrates optical power using electric power as a basis of comparison. It is suitable for high powers where there currently are a lack of opportunities and the calibration can be performed in room temperature. It covers a wide spectral area since the system measures temperature rise in the photodiode. The system is easy to use and it is easy to make changes on it.

Optical power has been calibrated using one optical voltage measurement and two electric voltage calibrations. The voltage difference generated by the optical power laid the basis for how much power that was needed from electric power. One electric calibration above and one below the voltage difference generated by the optical power source was done to determine an interval for where the optical power had to be. The interval was [4.93 mW 7.67 mW]. Using this and assuming that the power-voltage difference relationship is linear within the interval the optical power was determined to be 7.0921 mW. To compensate for reflective losses from the surface of the photodiode one must consider the reflected power. The reflected power from the surface with a normal incident angle was calculated to be R = 32.99%. The optical power now becomes 10.5836 mW which is the calibrated optical power. The system is accurate and can calibrate optical power down to 10^{-7} W.

The most problematic source of error is the noise. The noise probably arises from grounding issues in the electric setup but with high incident optical power the noise is less influential. Measures were taken along the way to reduce noise in the system. Replacing the potentiometers originally intended in the electric circuit proved very useful.

5.1 Future Work

Looking further on how to reduce noise in the electrical circuit to a greater extent could be an option on how to improve the system. Investigating the grounding issue should be prioritized. Looking at some alternative circuits and components and investigate if they can improve the system. The instrumentation amplifier could be replaced with an ultra-low noise instrumentation amplifier like this one [4].

Prospective tasks may also include elimination/minimizing reflection losses at the photodiode surface. This can be done by installing a mirror with a certain angle with respect to the photodiode as presented in section 2.7.2.

Improving the thermal design by a more robust and permanent setup would make it easier to reproduce the measurements. Replacing the existing photodiode with a pure silicon chip without the ceramic housing that make up the Hamamatsu photodiode would increase sensitivity, but it could be somewhat more susceptible to temperature fluctuations and air gusts from the environment. Protecting it properly would be important if this choice would be pursued. One could also enhance the current flow tolerance of the Hamamatsu photodiode, which has an upper limit of 500 mA. With an enhanced current tolerance one would be able to reach higher electric powers and hence, increase the range of which the system could calibrate optical power.

Bibliography

[1] Lakeshore Cryotonics CX 10xx model specifications. http://www.lakeshore.com/products/cryogenic-temperature-sensors/cernox/models/pages/Specifications.aspx.

[2] Photometry A National Measurement System for Radiometry and Pyrometry Based upon Absolute Detectors. http://www.nist.gov/pml/pubs/tn1421/index.cfm.

[3] Analog Devices. *AD620 Data Sheet.*

[4] Analog Devices. *AD8429 Data Sheet.*

[5] Ozcan Bazkir and Farhad Samedov. Electrical substitution cryogenic radiometer based spectral responsivity scale between 250-2500 nm wavelengths. 2004.

[6] Refractive Index Database. http://refractiveindex.info/legacy/?group=CRYSTALS&material=SiO2&option=Ghosh-o&wavelength=0.488.

[7] The Human Eye Sensitivity Function. http://en.wikipedia.org/wiki/Luminosity_function.

[8] J.L. Gardner and F.J. Wilkinsob. Angular effects in silicon photodiode responsivity comparisons. 1997.

[9] Martin A. Green. Self-consistent optical parameters of intrinsic silicon at 300 k including temperature coefficients. 2008.

[10] Hamamatsu. *Si photodiode S1337 series Data Sheet.*

[11] Texas Instruments. Noise analysis in operational amplifier circuits; application report, 2007.

[12] The Fabry-Perot interferometer. http://en.wikipedia.org/wiki/Fabry%E2%80%93P%C3%A9rot_interferometer.

[13] Art Kay. *Operational Amplifier Noise; Techniques and Tips for Analyzing and Reducing Noise*. Newnes, 2012.

[14] Keithley. *Keithley 2000 M Data Sheet*.

[15] Lakeshore Cryptonics. *CX-1070 Data Sheet*.

[16] J.E. Martin. A cryogenic radiometer for absolute radiometric measurements. 1985.

[17] Farshid Manoocheri Meelis Sildoja and Erkki Ikonen. Reflectance calculations for a predictable quantum efficient detector. 2009.

[18] Rs-5900 Electrically Calibrated Pyroelectric Radiometer. http://www.laserprobeinc.com/Rs5900.pdf.

[19] B. E. A Saleh and M. C. Teich. *Fundamentals of Photonics*. Wiley, 2007.

[20] Norwegian Metrology Service website. http://www.justervesenet.no.

Appendix A

Fitted Curves

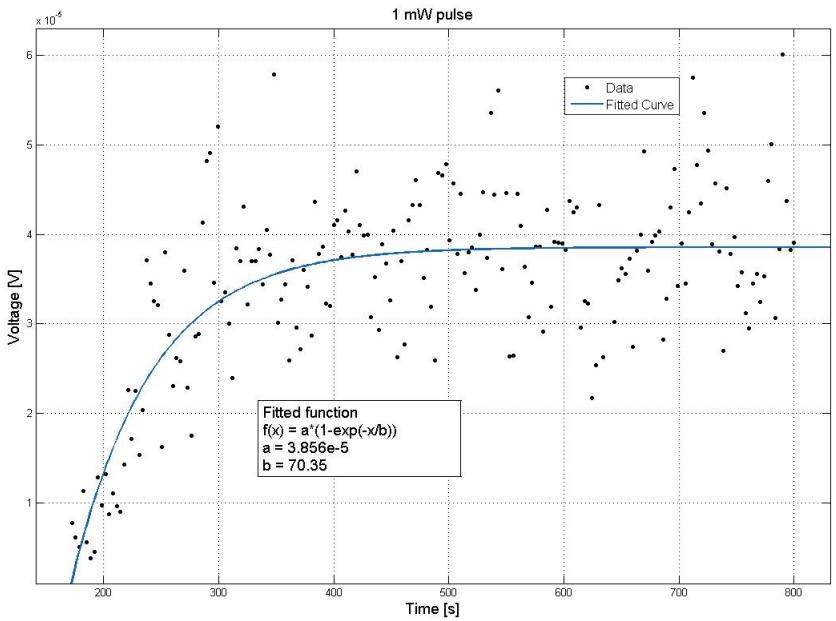

Figure A.1: Fitted curve of the 1 mW pulse.

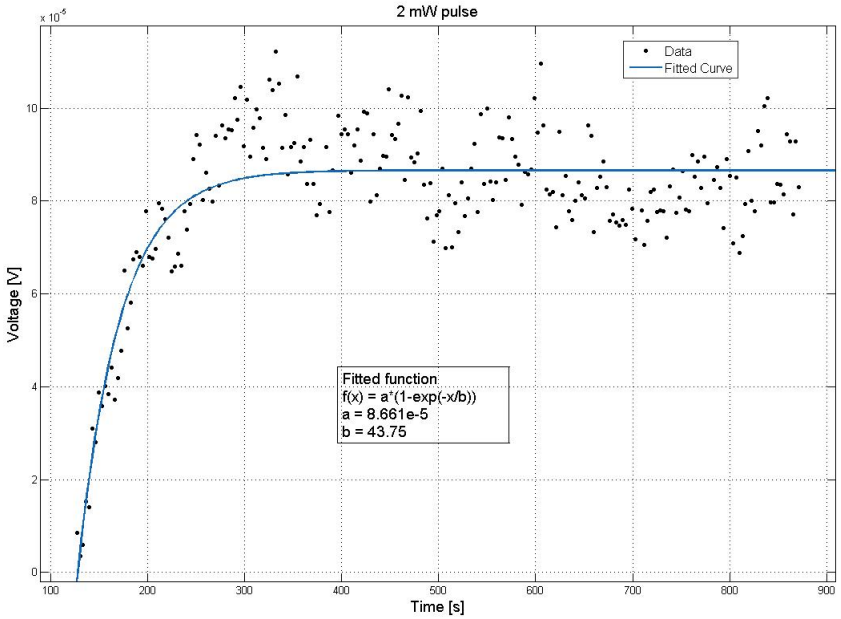

Figure A.2: Fitted curve of the 2 mW pulse.

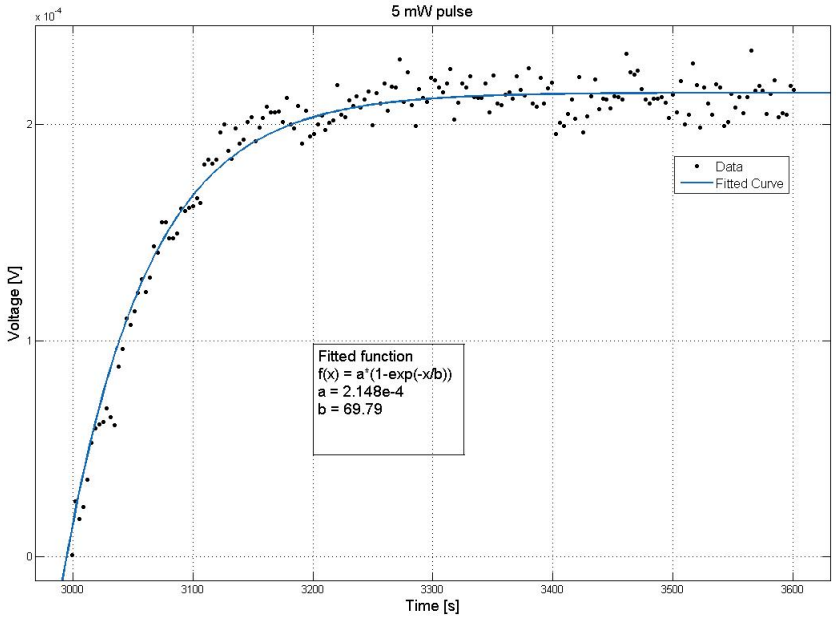

Figure A.3: Fitted curve of the 5 mW pulse.

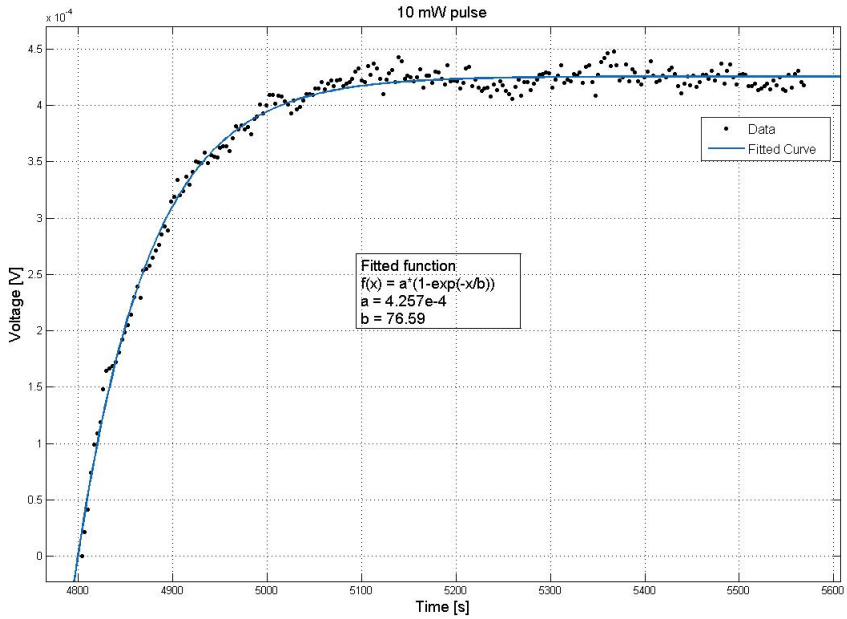

Figure A.4: Fitted curve of the 10 mW pulse.

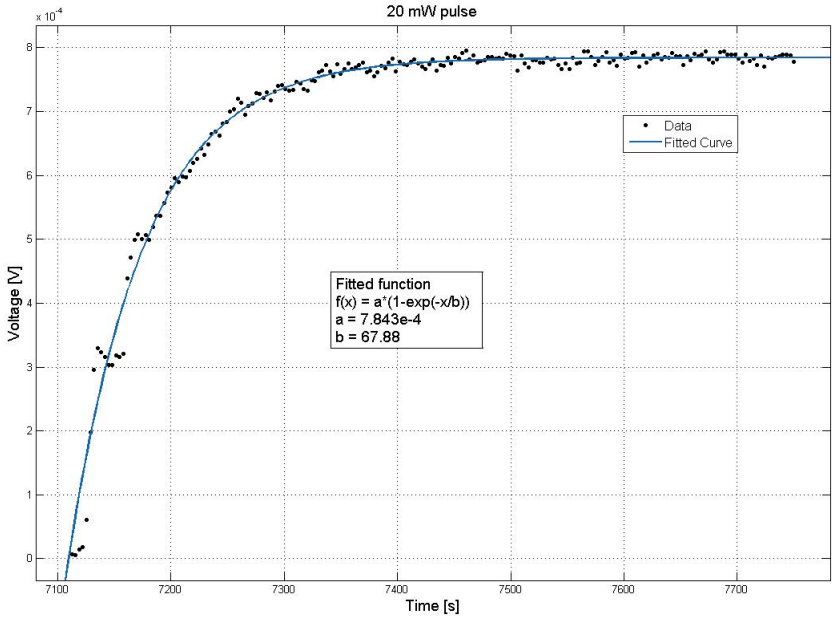

Figure A.5: Fitted curve of the 20 mW pulse.

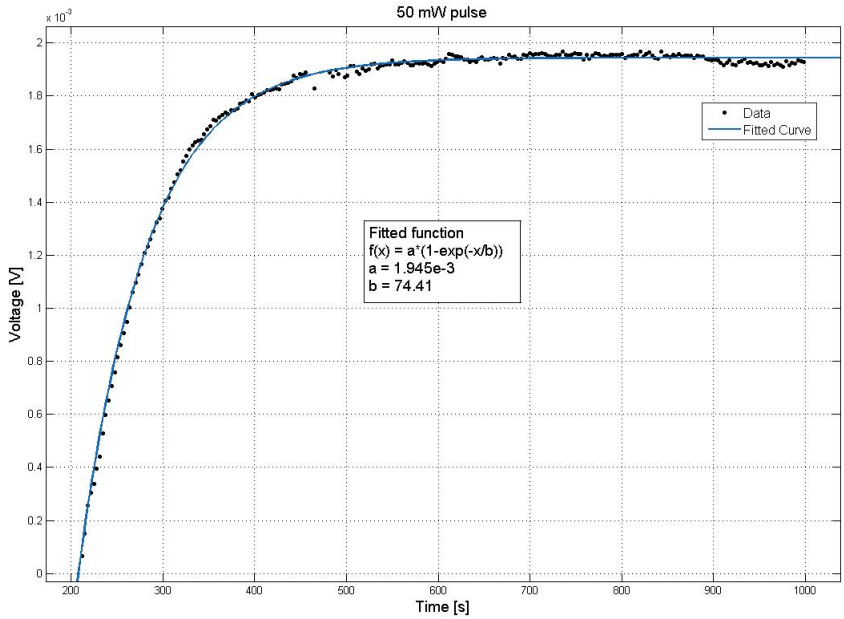

Figure A.6: Fitted curve of the 50 mW pulse.

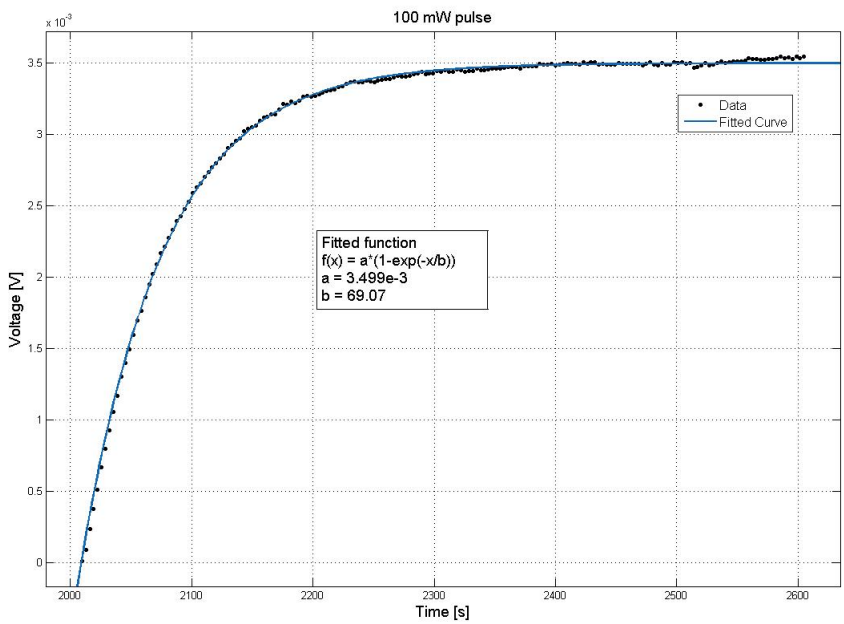

Figure A.7: Fitted curve of the 100 mW pulse.

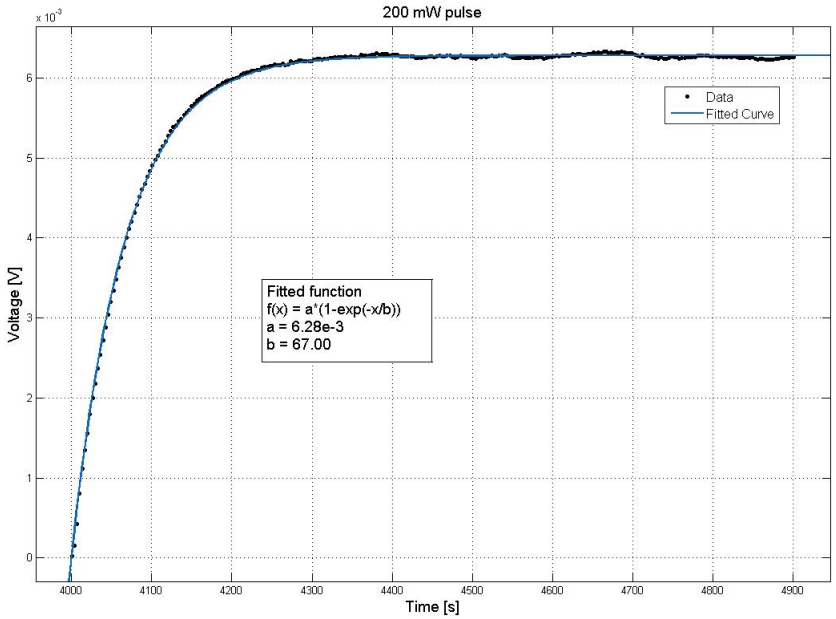

Figure A.8: Fitted curve of the 200 mW pulse.

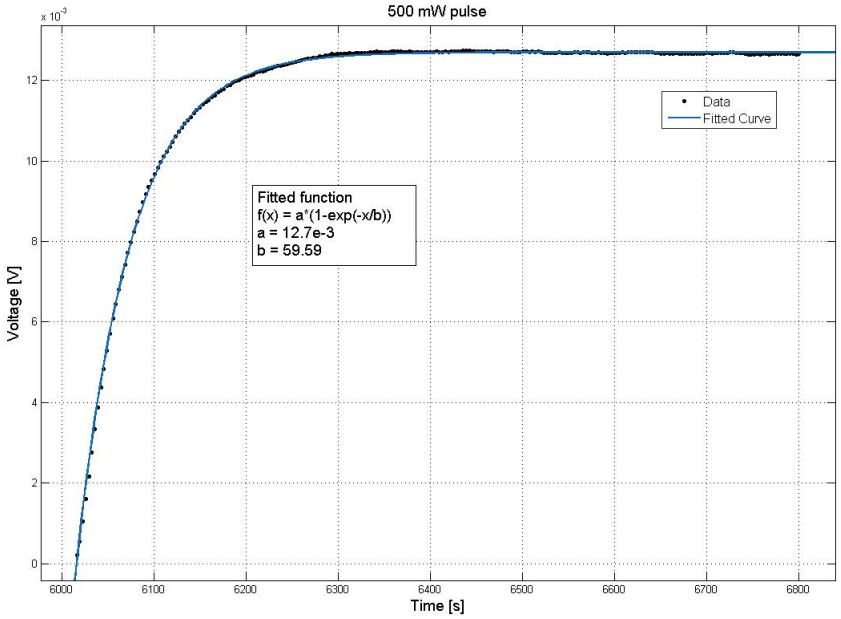

Figure A.9: Fitted curve of the 500 mW pulse.